SEQUENCING AND DETERMINATION OF HORIZONTAL WELLS AND FRACTURES IN SHALE PLAYS: BUILDING A COMBINED TARGETED TREATMENT SCHEME

A. Alzahabi, M. Soliman, G. Asquith, G. Al-Qahtani
Texas Tech University

ABSTRACT

This paper introduces a new design and validation of a new integrated combined Fracturability index correlation. Ultra-low formation permeability has dictated the creation of a large number of fractures from a single horizontal well. It is not uncommon to design a horizontal well with more than one hundred hydraulic fractures transversely intersecting the horizontal well. The large number of fractures is driven by the short exploitation distance resulting from the nano-darcy formation. Fracturing horizontal wells results in creating of a larger volume of improved reservoir quality. The term SRV is used to describe this improved volume. Mayerhofer et al. discussed the concept of SRV in a recent publication. Methods to manipulate fracturing sequence to enhance fracture complexity and consequently enlarge and enhance the stimulated reservoir volume have been developed by several authors (East et al 2010). Discussion on the background is found in papers by Soliman, et al. (2008), Soliman et al. (2010), and Roussel and Sharma (2011).

INTRODUCTION

Bowker (2003) determined that the majority of the production in the Barnett Shale comes from zones with 45% quartz content and only 27% clay. Wang and Gale (2009) and Jarvie et al. (2007) introduced a brittleness index defining ductile and brittle regions in terms of mineralogical analysis. Yu et al. (2013) used an economic optimization to identify the optimum parameters of fracture conductivity and distance between two neighboring wells based on Barnett.

However, the well-known heterogeneity of shale plays is another very important criterion that has a direct impact on how a shale play should be exploited. The presence of natural fractures, as well as heterogeneity in geomechanical, petrophysical and geochemical properties, impacts the utilization of shale plays. Stegen, et al. (2012) and Cipolla, et al (2010, 2012), among others, have hypothesized that at least 50% of created fractures do not contribute significantly to the total production. This observation indicates that the process of uniformly spacing the fractures or even the horizontal wells does not yield the optimum utilization of a shale play three issues are therefore necessary to address:

1. Defining a representative shale sweet spot indicator.
2. Locating and optimization of the process of locating horizontal wells in a shale play.
3. Locating and optimization of the process of locating hydraulic fractures in a horizontal well.

The third issue of locating fractures has been discussed by several authors. Rickman et al. (2008) defined a new brittleness based solely on Young's Modulus and Poisson's ratio. By use of this brittleness index, various areas in a shale play may be divided into brittle and ductile areas. Fractures would be recommended in the areas defined as brittle. Figure 1 shows the graph by Rickman et al. indicating the distribution of brittle and ductile areas of the shale plays in areas examined by Rickman et al.

Recently, Mullen et al. introduced a more complex Fracturability Index. The primary rock property input in their work is brittleness as directly correlated with Brinell hardness. Mullen et al. determined that zones where proppant embedment is less likely and where the rock is more likely to create a complex fracture network have a high Fracturability Index value.

Parker et al. (2009) used well logging to show the variation in Young's modulus and Poisson's ratio along a Haynesville shale horizontal. Parker et al. used the criteria developed by and Rickman et al. and Mullen et al. to locate the relatively brittle areas along the horizontal. The brittle areas were selected for fracturing.

Numerous authors have developed various indices to define areas of fracturability. While helpful in approximating future locations of planned fractures, such approaches tend to focus on one area of technology. None of those techniques consider all the possible parameters that may affect fracture placement and propagation.
Optimization methodologies are being developed for fast tracking the number of fractures and the number of effective horizontal wells in shale plays by a fast and effective method. The sequencing of well and fracture placement is key to achieving economical utilization of shale assets in North America. Of critical importance are the computational methods used for optimization of placement.

While equally important, the second issue that of locating horizontal wells in unconventional reservoirs to take advantage of sweet spots, has not received appropriate attention. Serious consideration of this issue has been presented by Alzahabi et al (2014). In their study work, Alzahabi et al. consider the petrophysical, geomechanical, geochemical and physical properties of the rock in the screening and placement of the fracture and develop a candidate evaluation algorithm.

The designed algorithm explores geomechanical, petrophysical and geochemical parameters of a newly discovered shale resource to provide a guiding database of major productive shale plays in North America, noting any potential for newly discovered shale plays. Their work is based on a built-in shale success factor, a factor which depends on statistics, database structure, candidate evaluation approach and the developed algorithm. The data structure of their algorithm consists of Shale Play Spider Plots, Completion Strategies, Mineralogy Comparison, Mechanical Properties, Characteristics, Shale Gas Production Indicators, and Sweet Spot Identifiers. The algorithm design contains characteristics and strategies to identify similarities to prioritized shale parameters and predict the likelihood of similarity, then recommending future development approaches. Clusters of checking maturity parameters, similarity, then rank and guide, are the main root model parameters. A procedure to redefine the groupings to create clusters that better represent the data is a new insight of this work, in addition to prediction of new basin performance based on the performance of proven basins. This procedure will help identify of sweet spots in new basins and will guide fracturing and well placement in shale plays.

Due to variations in mechanical, geochemical, and geomechanical properties which occur on the level of a few inches in the shale model, the planning of clusters should not involve their common even distribution. The effect on production is significant when the whole process is optimized.
Figure 3 shows a common design in horizontal wells which can be implemented using the perf and plug approach. This design accommodates as many e fractures as possible, to achieve maximum contact surface. At this point, it is pertinent to address envisioned methods of selectively fracturing and selectively plugging.
Figure 4 shows a comparison between equally spaced clusters within the stage and (at right) FI drove-placed clusters. The math demonstrates that the conventional approach is preferable. But the accurate basin modelling tells a new and different story guided by the newly developed Fracturability Index (FI) approach, applicable with brittle versus ductile rock, naturally fractured rock versus none, and very heterogeneous versus uniform properties.

The developed technology:

Achieving maximum contact area with high quality points within the model is possible, where optimization of vertical and deviated well placement help in achieving better access to good quality points. The quality of the shale resource comes from brittle and high TOC content. The key is to allow representative factors to guide optimization algorithms. Adapting the resource model can benefit placement and guide fracture positioning in any shale play.

The technology takes into account various elements such as size, time, and number. In contrast to current thought in the industry, which posits that more fracture is better, we are developing a technology suggesting that the effective fracture is better. Effective fractures are those that target brittle zones in the shale basin, resulting in branched fractures and deep encroachment into virgin parts of the model.

DATA ANALYSIS:

We researched the change in many parameters effect of geomechanical properties (Poisson's ratio and Young's Modulus on Fracturability Index).

Insights of the above three figures:

- Both E and PR affect FI
- There is a relationship between FI and E within a certain range

As A result of new ways of understanding the rock, fluid and interactions, our ability to design treatment will not be limited. Standardizing the treatment process with newly developed indices facilitates the initiation of fracture in shale according to a planned, automated process.

An integrated mix of high-resolution seismic, accurate sonic, and formation imaging is the main enabling tool for detailed basin description. Structural features can be translated into quantified ranges, which should be filtered within the algorithm to subcategories. The classifications include *very good brittle, brittle, ductile* and *very good ductile*.

Developing an integrated Fracturability Index correlation:

The main parameters of rock are as follows:

Independent variables: Plane Strain Young's Modulus, Mineralogical Brittleness Index

Dependent variables: Fracturability Index = Normalized Strain Energy Release

The term "Gc" is the critical energy release rate; it is related to Ua, or energy per fracture area.

$$G_c = 2\,U_a \tag{1}$$

$$U_a = \frac{{K_{Ic}}^2}{4\mu(1+v)} \tag{2}$$

Equation 1 and 2 after Wickham, J. et al. (2013)

The energy released in creating fractures is approximately equal to the energy required to create it.

First Correlation:

$$\mathrm{FI} = \mathrm{Gc_n} = \frac{\mathrm{Gc} - \mathrm{Gc_{min}}}{\mathrm{Gc_{max}} - \mathrm{Gc_{min}}} \tag{3}$$

$$\mathrm{Gc} = \frac{{\mathrm{K_{IC}}}^2}{\mathrm{E}} \tag{4}$$

$$\mathrm{FI} = 10^{\left(\mathrm{a+b\times log}\left(\frac{1}{\frac{E}{1-v^2}}\right)+\mathrm{c\times log}\left(\frac{\mathrm{quartz+Pyrite}}{\mathrm{quartz+Pyrite+Clay+Calcite}}\right)\right)} \tag{5}$$

	Coefficients
A, Intercept	14.41832
B	2.034596
C	0.065136
Regression Statistics	
Multiple R	0.98

The first correlation is built on concept of the critical energy to create a fracture, as an example Fracturability Index (FI) ≥ 0.41 indicates higher energy required which stands for poor rock. On the other hand, FI≤ 0.41 indicates less energy required which stands for brittle rock.

Second Correlation:

The energy release rate failure criterion states that a crack will grow when the available energy release rate exceed the critical energy release rate value.

$$G = \frac{\partial(U-V)}{\partial A} \tag{6}$$

Where U is the potential energy available for crack growth

V is the work associated with any external forces acting in the crack area (crack length for two-dimensional problems)

G unit is in $\frac{J}{m^2}$

$$G \geq G_c \tag{7}$$

G_c is the critical value and fracture energy

$$G = \frac{K_I^2}{E'} \text{ (Assume plane strain)} \tag{8}$$

$$K_I = 0.313 + 0.027 \times E \quad \text{Correlation} \tag{9}$$

Then substitute eqn. 4 in eqn. 3

$$G = \frac{K_I = [0.313 + 0.027 \times E]^2}{E'} \quad \sim \quad \text{E} \tag{10}$$

$$G \propto E \tag{11}$$

$$FI = B_0 \times 10^{[B_1 + B_2 \times log\left(\frac{1}{MFI}\right) + B_3 \times log(E')]} \tag{12}$$

Where E in psi

MFI= Mineralogical Index

Higher E~ but the better the resultant fracture, the more energy is required for the growth.

$$G \propto E$$

The more brittle quartz is in composition and the easier to fracture, the less energy is required

$$G \propto \frac{1}{MBI} = \frac{Quartz + Feldspar + Pyrite + Dolmoite + Calcite}{Quartz + Feldspar + Pyrite} \tag{13}$$

Consider the following:

- The energy that is consumed by creating a new surface should be balanced by the potential energy of the system.
- $dW_{elas} + dW_{ext} + dW_s + dW_{kin} = 0$
- dW_{elas} represents the change in elastic energy stored in the solid,
- dW_{ext} is the change in potential energy of exterior forces,
- dW_s is the energy dissipated during the propagation of a crack,
- dW_{kin} is the change in kinetic energy,
- Applying the Griffith criterion for fracture initiation and growth,

Figure 1: The relationship between Young's Modulus and Quartz of Wolf Camp Formation

B_0	10^{-6}
B_1	-0.233205322

B_2	-0.032424691
B_3	1.009850946

$$FI = B_0 \times 10^{[B_1 + B_2 \times \log\left(\frac{1}{MFI}\right) + B_3 \times \log(E')]} \quad (14)$$

The second correlation is built on concept of the needed energy to create a fracture, as an example Fracturability Index (FI) = 7 indicates higher energy required which stands for ductility. On the other hand, FI=2 indicates less energy required which stands for brittle rock.

An alternate industry-used approach for locating sweet spots:

In this section, we establish a new integrated approach for understanding unconventional rock, including geomechanical parameters and detailed mineralogy of the reservoir.
The new integrated FI takes both geomechanical and geochemical effects into consideration.
Three categories are distinguished: *highest, high zones, and bad zones*.
The new classification identifies the shale reservoir based on brittleness, high porosity, and organic material. In creating our new correlation, we made use of the results of a study by Walls et al. (2012). With his own developed criterion as a separate scale for checking sweet spots using developed FI in Permian Basin shale reservoirs, they used 16 core samples from Eagle Ford, located in Maverick, Dimmit, LaSalle and Atascosa counties in South Texas, USA. Pore and grain scale results were used to obtain information on porosity distribution, organic material volume, and organic material pore structure.
For shale reservoirs, a *Sweet Spot* refers to those portions of the basin that have high porosity, highly brittle composition, are high in organic matter and easier to fracture. The higher the porosity is, the greater the maturity.
Density and PEF from Dual-Energy CT allowed independent verification of our data for sweet spot portions. Then we used mineralogical and geomechanical principles to construct the new correlation. The highest category contains high porosity, high Kerogen and a composition of quartz; the second in rank contains high porosity, high Kerogen and a composition of calcite after Lewis et al (2013) and Schlumberger.

1. Highest category sweet spot zones, has bulk density (RHOb) < 2.53 and photoelectric index (Pe)<4.0
2. High category sweet spot zones, has bulk density RHOb < 2.53 and Pe>4.0
3. Low category sweet spot zones: the remaining data

Photoelectric index (PE) for Mineral Identification:

The photoelectric index (PE) is a measurement by modern logging tools to measure the absorption of low-energy gamma rays by the formation in units of barns per electron. Significant here is the difference between main reservoir rock-forming minerals quartz (PE= 1.81 barns electron^{-1} , calcite (PE= 5.08 barns electron^{-1}), dolomite ((PE= 3.14 barns electron^{-1}), Montmorillonite ((PE= 2.04 barns electron^{-1}), Kaolinite ((PE= 1.49 barns electron^{-1}), Illite ((PE= 3.45 barns electron^{-1}), Chlorite ((PE= 6.3 barns electron^{-1}) and oil ((PE= 0.12 barns electron^{-1}) (for more details, see *Physical properties of rocks : a workbook* by J.H. Schön 2011).

Combining both techniques for sweet spot identification:

Table 2 introduces the recommendation list of shale sweet spot classification according to the developed index (this paper) versus that of Walls.

Figure 7 explains the developed sweet spot selection methodology.

Figure 8 demonstrates a geomechanical based FI correlation introduced by Alzahabi et al. 2015.

Figure 9 demonstrates the relationship between the second developed Fracturability Index versus plane strain young's modulus.

Figure 10 demonstrates the relationship between the second developed Fracturability Index versus Mineralogical brittleness Index.

Figure 11 shows the preferred facies which is organic siliceous shale and organic mixed shale as introduced by Wang & Carr, 2013. Figure 11 also shows shale lithofacies after Wang & Carr, 2013.

Figure 12 shows a classification of four categories of sweet spot regions after Walls et al. 2012. The red and green indicate recommended sweet spot locations of shale.

Figure 13 shows Shale Lithofacies classification after Wang & Carr, 2013

The scientific reason why density and PE, both is a direct indicator of formation lithology.

Figure 15 through 16 show a testing to the data using our three devolved criteria versus the criteria developed by Walls et al 2012.

Study Area:

The area of study is located in the Midland area, Permian Basin shale Wolf Camp formation. The Wolf Camp is dominated by organic-rich and siliceous lithofacies. Its detailed description is included in Table 3 and in Figure 14.

Testing and validation of the work: (Permian Basin Wolf Camp Shale Reservoir Data):

Table 4 lists the testing process of the two criteria used in classifying the shale reservoirs. The next section offers a detailed explanation of how this developed integrated FI can be used to guide fracture and wells in a sequence.

Figures 15 and16 show application of the criteria on the tested model.
Figures 17 through 21 demonstrate detailed application of the developed approach, starting with S1, S2, and S3, matching all criteria to suggest the best horizontal well path. The result of this testing indicates that it is preferable to locate wells in the sweet spots of the reservoir, where quartz is abundant, which facilitates the drilling and locating of fractures, and where hydrocarbons are concentrated. It is also supported that sweet spot portions of rock occur where horizontal stress is minimum and differential horizontal stress ratio is maximum, as explained later in this paper.

DIFFERENTIAL HORIZONTAL STRESS RATIO (DHSR):

Net Pressure and Stress

Using net pressure data, we can gain an idea about the difference between maximum and minimum stress.

Nolte Smith provided a simple equation for fissures opening

$$P_o = \frac{\Delta\sigma_h}{(1-2\,\nu\,)} \tag{15}$$

Differential Horizontal stress ratio (DHSR), a scale used for placing horizontal wells, is very important in deciding whether a selectively chosen region in a shale play will fracture easily or not. It can be obtained from Seismic data alone.

A planned fracture is believed to exist when designing fracs in high quality relative points of DHSR. We used the following formula to calculate DHSR.

$$DHSR = \frac{\max Stress - \min stress}{\max stress} \tag{16}$$

Figure 23 illustrates the differential horizontal stress profile. This plot suggests placing the horizontal well in the interval 8,300-8,400 ft.

HYDRAULIC FRACTURING STAGE SEQUENCING:

With many wells (ranging from 5 to 40) originating from one pad as a surface location, a common successful scenario involves *simulfrac*), which is the fracturing of stages simultaneously on parallel wells; the second approach involves alternating stages between adjacent parallel wells (Zipper Frac); the third (recently developed) is Modified Zipper Frac. These approaches are successful in utilizing the surface equipment and developing a larger surface area in shale and tight formation. The key behind these approaches, is that the rock between wells may have a superposition of stress which can help in effective stimulation of tight rocks. Many micro-seismic results show that second and third stages are less effective than the first treatment even if the same fluid volume and proppant amount are injected.

This paper introduces a new fracturing methodology called Cascade Fracturing Technology. This methodology starts by dividing the well path into segments, identifying the order of fracture locations along the well path and ordering the fractures from the production point of view. This methodology is followed for all wells in the reservoir, thus prioritizing the completion strategy. Results show that shale reservoirs may be produced more effectively by using this new methodology. In addition, the number of fracture stages designed by use of the new fracturability index is lower than by use of conventional techniques, thus reducing the cost of fracturing. The timing of fractures, number of fracture stages, clusters for each stage, and number of wells may be determined based on reservoir and fluid properties rather than by trial and error approaches. Figure 24 shows a schematic that follows the suggested design after sequencing by the newly developed FI.

Figure 26 shows a map of the FI calculated for the tested shale model using correlation by Alzahabi et al. 2015.
Figure 27 shows an optimized placement of wells and fractures in the same model.
Figure 28 shows the sequencing approach developed by this work, where FI values suggest the cascade fracturing approach through order of fracture placement stages.

CONCLUSIONS

The developed work is a new sweet spot guide, designed primarily for placement of deviated wells and fracture stages in shale resources. Issues such as height growth and variations in rock mechanics have been extensively checked here.

In conclusion, the issues of well and fracture placement and optimization require more focused attention than they currently receive. Increased attention to this area of investigation should lead to more economical development of shale plays.

Currently, it is well known that fracture gradient and in-situ stress along the path are not the same. We therefore recommend that each single stage should follow a certain method of fracturing, and every single cluster of perf should be consistent.

Two new screening criteria are being developed for identifying sweet spot locations with shale reservoirs.

An agreement has been obtained for locating the horizontal wells between FI, S1, S2, and DHSR, a promising indication that the new criteria can be used for future well placement and fracture allocation.

NOMENCLATURE

FI Fracturability Index
E Young's Modulus, psi
E' Plane Strain Modulus, psi
$E_n{}'$ Normalized Plane Strain Modulus
ν Poisson's ratio
ρ Density, lb. /ft^3
$x_{(i,j)}$ X_Y location of a fracture in the reservoir represents the location *(I, j)* in the shale formation grid
X Coordinate axis along well path, ft
Y Coordinate axis along fracture path, ft
BHP Bottomhole pressure, psi
Q_g Gas flow rate, Mscf/d

c_f Formation compressibility, psi^{-1}
L_f Fracture half length, ft.
Pi Initial reservoir pressure, psi
L Well Lateral length, ft.
$\Delta X, \Delta Y$ Model grid dimensions in x and y direction, ft.
P_{net} Net pressure, psi
X_e, Y_e Rectangular Reservoir shape dimensions in x and y direction, ft.
W Horizontal well
F Fracture stage
D_{min} Min well spacing, ft.
G_c Critical energy release rate
U_a Energy per created fracture area.
$\emptyset$ Porosity

REFERENCES:

Alzahabi, A., AlQahatani G.D Soliman, M. Y., Bateman, R., and Asquith, G. (Jan. 2015) "Fracturability Index Maps for Selectively Enhancing Fracture Propagation in Shale Plays" Hydraulic Fracturing Journal, Volume 2-No.1,.

Alzahabi, A., Mohamed, A., Soliman, M. Y., Bateman, R., and Asquith, G. (2014) Shale *Plays* Screening Criteria, A Sweet Spot Evaluation Methodology. Fracturing Impacts and Technologies and Conference September 4-5, 2014, Lubbock, TX

Cipolla, C. L., Maxwell, S. C., & Mack, M. G. (2012, January 1). Engineering Guide to the Application of Microseismic Interpretations. Society of Petroleum Engineers. doi: 10.2118 / 152165-MS

East, L.E., Soliman, M.Y., and Augustine, J.R. (2010). Methods for Enhancing Far-Field Complexity in Fracturing Operations. *SPE Production & Operations* (3): 291–303.

Griffith, A. A., 1921, "The Phenomena of Rupture and Flow in Solids," Philosophical Trans. Royal Society, London, Vol. A221, pp. 163-198.

http://www.engineerlive.com/content/23507

Jarvie, D., M., Hill, R.J., Rube, T.,E., and Pollastro R.M. (2007),Unconventional shale-gas systems: The Mississippian Barnett Shale of north-central Texas as one model for thermogenic shale-gas assessment, AAPG Bulletin, V. 91, No. 4, DOI:10.1306/12190606068.

Lewis, R. (2013) American Association of Petroleum Geologists, Basic Well Logging School, course notes, Golden Colorado.

Mayerhofer, M.J., Lolon, E., Warpinski, N.R., Cipolla, C.L., Walser, D.W., and Rightmire, C.M. (2010). What Is Stimulated Reservoir Volume? *SPE Production & Operations* (1): 89–98.

Miller, C., Waters, G. and Rylander, E. (June 2011), "Evaluation of Production Log Data from Horizontal Wells Drilled in Organic Shales" SPE 144326, presented at the SPE NAUGCE, Woodlands, Texas, USA.

Mullen, M. and Enderlin M.(Oct. 2012.) "Fracturability Index – More Than Just calculating Rock Properties" SPE paper 159755, presented at the SPE Annual technical Conference, San Antonio, TX., USA.

Nolte, KG. ans Smith, M.B. (1981):"Interpretation of Fracturing Pressure," JPT, September, SPE 1767.

Oil Field Review Summer (2013), Stimulation Design for Unconventional Resources: 25, no. 2.

Parker, M., Petre, J. E., Dreher, D. (2009). Haynesville Shale: Hydraulic Fracture Stimulation Approach, paper-0913 presented at the International Coalbed &Shale Gas Symposium, Tuscaloosa, Alabama.

Rickman, R., Mullen, M. J., Petre J. E. et al. (2008). A Practical Use of Shale Petrophysics for Stimulation Design Optimization: All Shale Plays Are Not Clones of the Barnett Shale. SPE Paper 115258, SPE Annual Technical Conference and Exhibition (ATCE), Denver, Colorado, USA, Sept 21-24.

Ron Schmid and Franck Delbecq, (2012). "Wide-azimuth seismic enables better shale play economics" E and P magazine, Shale reservoir characterization in the Haynesville, October.

Roussel, N.P. and Sharma, M.M. (2011). Optimizing Fracture Spacing and Sequencing in Horizontal-Well Fracturing. *SPE Production & Operations* (2): 173–184.

Schön, J., H., 2011. Physical properties of rocks: a workbook: Handbook of Petroleum Exploration and Production, 1st edition, Vol. 8. Elsevier.

Soliman, M.Y., East, L.E., and Adams, D. (2008). Geomechanics Aspects of Multiple Fracturing of Horizontal and Vertical Wells. *SPE Drilling & Completion* (3): 217–228.

Soliman, M.Y., East, L.E., and Augustine, J.R. (2010). Fracturing Design Aimed at Enhancing Fracture Complexity. Paper SPE 130043-MS presented at The SPE EUROPEC/EAGE Annual Conference and Exhibition, Barcelona, Spain, 14–17 June.

Stegent M., Wagner A., Stringer C., Tompkins R. and Smith N. (2012), "Engineering Approach to optimize Development Strategy in the Oil segment of the Eagle Ford Shale: A case Study" SPE 158846 presented at the SPE ATCE, San Antonio, Texas, USA.

Walls, J., B. Driskell, S.W. Sinclair, & J. Devito, (2012), "Reservoir Characterization in the Eagle Ford Shale using Digital Rock Methods": WTGS2012 Fall Symposium, Publ. No. 12-125.

Wang, F. P., and Gale, J. F. W. (2009) Screening Criteria for Shale-Gas Systems: Gulf Coast Association of Geological Societies Transactions, v. 59, p. 779-793.

Wickham J., Yu X., McMullen R., (2013) "Geomechanics of Fracture Density" URTeC ID 1619745 presented at the Unconventional Resources Technology Conference , Denver, Colorado, USA, 12-14 August.

Yu et al. (2013), "Optimization of Multiple Hydraulically Fractured Horizontal Wells in Unconventional Gas Reservoirs", Journal of Petroleum Engineering, Vol. 2013, Article ID 151898.

Table 1: An example of classified sweet spots by Walls et al. (2012)

High porosity	and /or Kerogen	More Quartz
Lower porosity	or Kerogen	More calcite
Lower porosity	or Kerogen	More calcite
Lower porosity	or Kerogen	Less calcite

Table 2 : Recommendation for sweet spot identifiers and shale classification.

Category	**Classification**	**FI, First Correlation**	**FI, Second Correlation**	**P_e & ρ_b**
Highest category sweet spot zones	S1	0.64-1.00	2.50-4.80	ρ_b< 2.53 and P_e <4.0
High category sweet spot zones	S2	0.41-0.64	3.60-5.20	ρ_b< 2.53 and P_e >4.0
Low category sweet spot zones	S3	0-0.41	5.20-7.00	The rest of data

Table 3: Data ranges used for testing the new criteria

Input parameters	
TOC, wt. %	2.3
RO	1.3
Total porosity, %	10
Net thickness, ft	1400
Adsorbed Gas	N/A
Gas Content	N/A
Depth, ft.	10100-11500 ≈10800
E, PR	4.6 E+6, 0.238
Mineralogy	Quartz, Feldspar, 61 % Clay, 30 % Pyrite, 1% Carbonate, 6.28 % Kerogen, %

Table 4: Checking for sweet spots using two scales

1st criteria , Rhoz<2.53 g/cc and Pe>4	**2nd Criteria Rhoz <2.53 g/cc and Pe<4**
yes	No
yes	No
yes	No
No	No
No	No
No	No
No	No
No	No
No	No
No	No

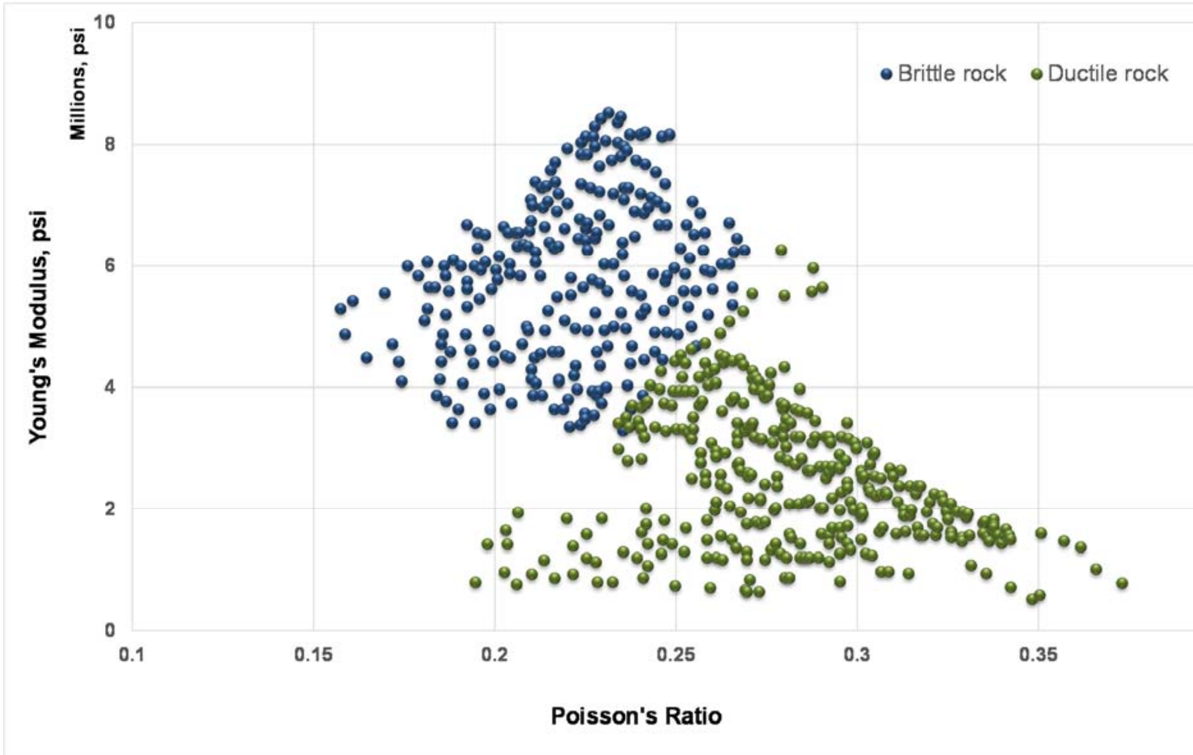

Figure 1 – Brittleness index after Rickman et al.(2008)

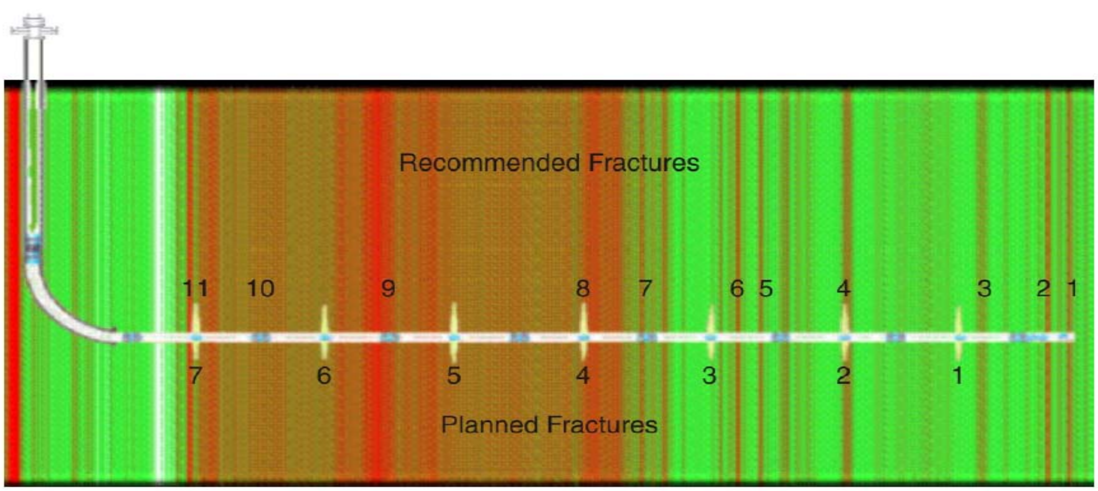

Figure 2- The brittleness track shows variation in rock heterogeneity, the red section is more brittle after parker et al. (2009)

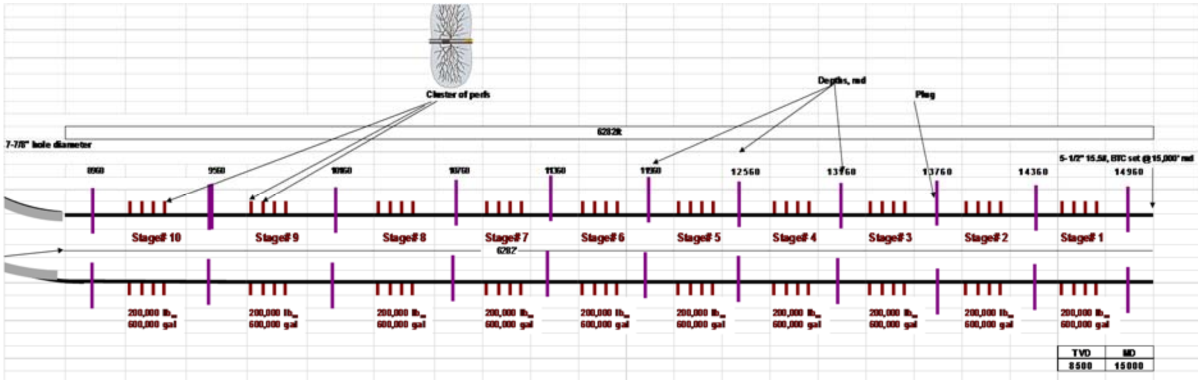

Figure 3: Common used approach of placing fractures in horizontal wells

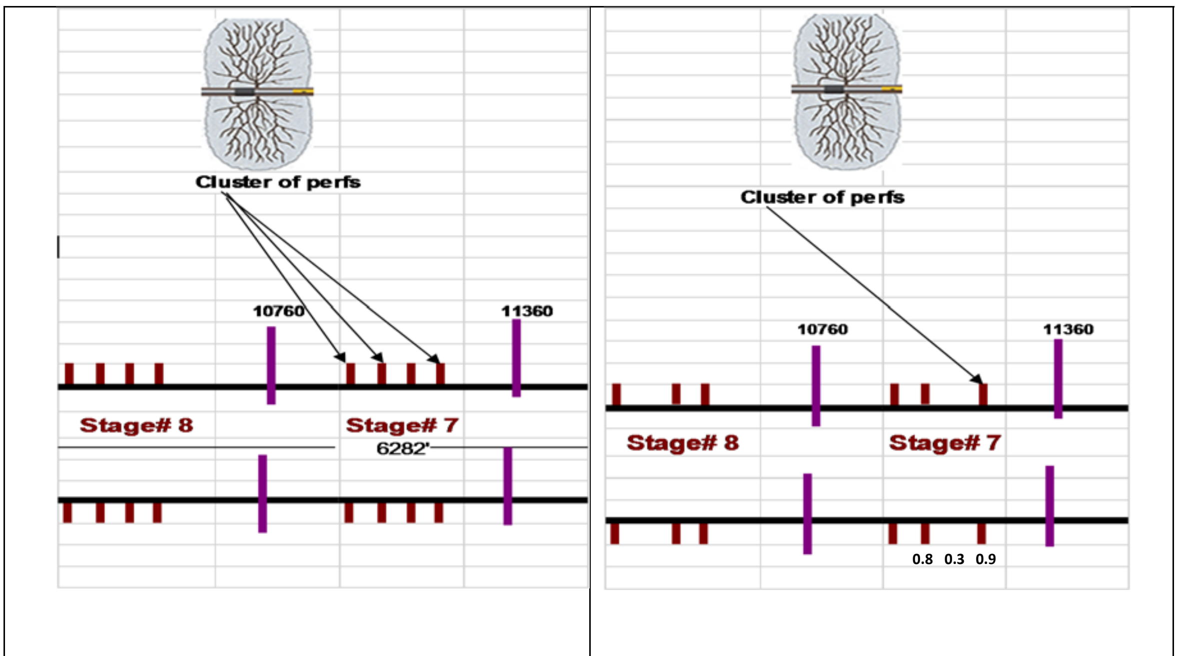

Figure 4: Comparison between equally spaced clusters within the stage and the one in the right shows FI drove placed clusters.

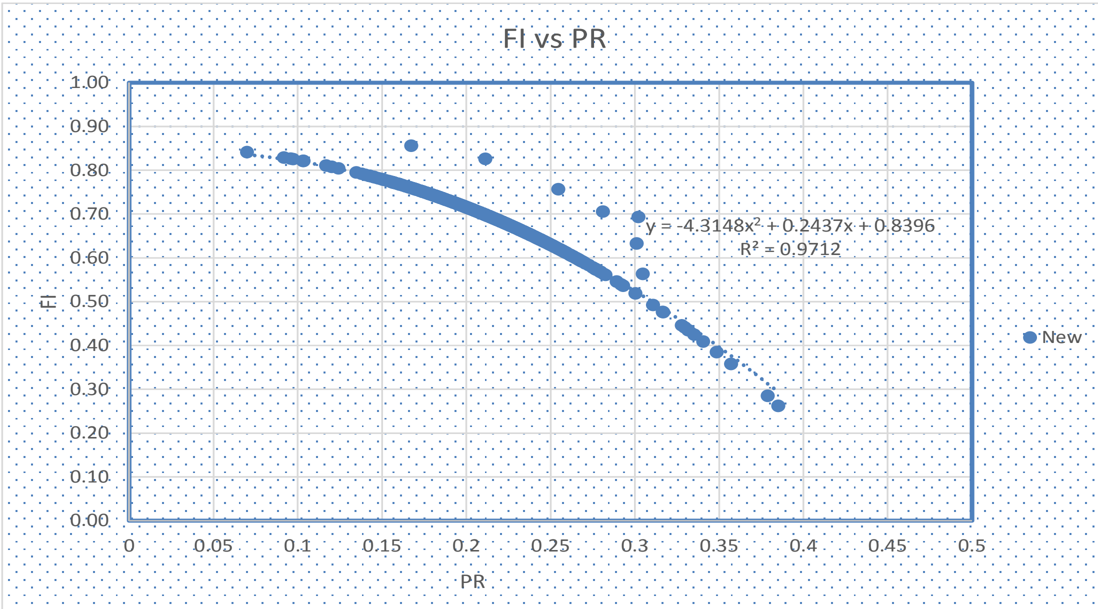

Figure 5: Effect of Poisson ratio on FI

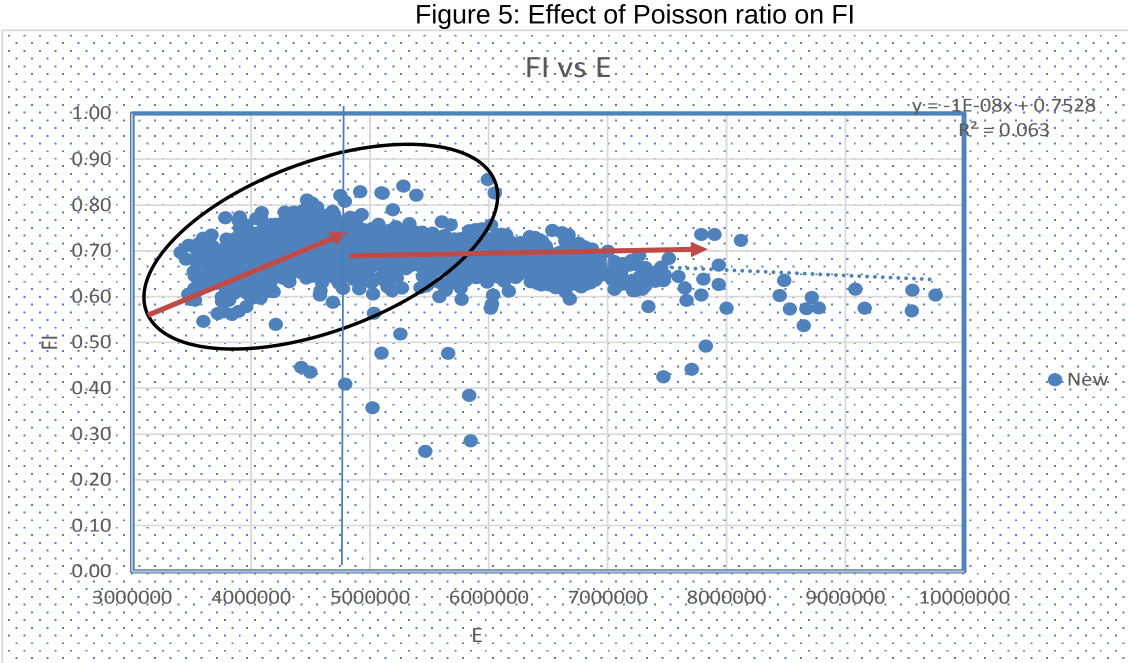

Figure 6: Effect of Young's Modulus on FI

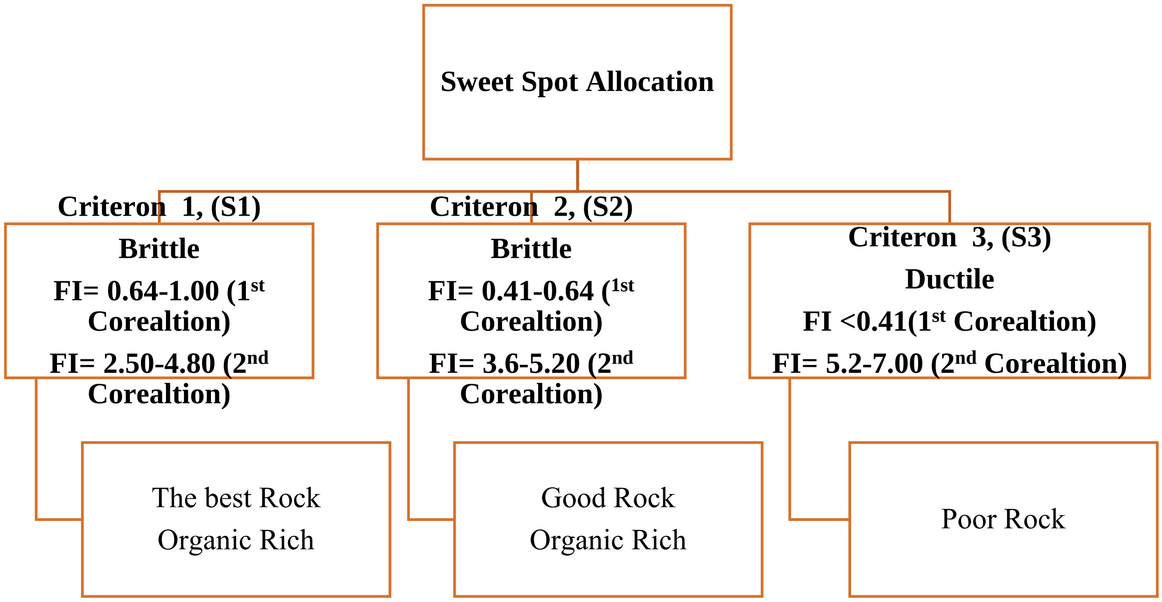

Figure 7: The developed sweet spot selection methodology for placing wells and fractures in shale reservoirs (this paper)

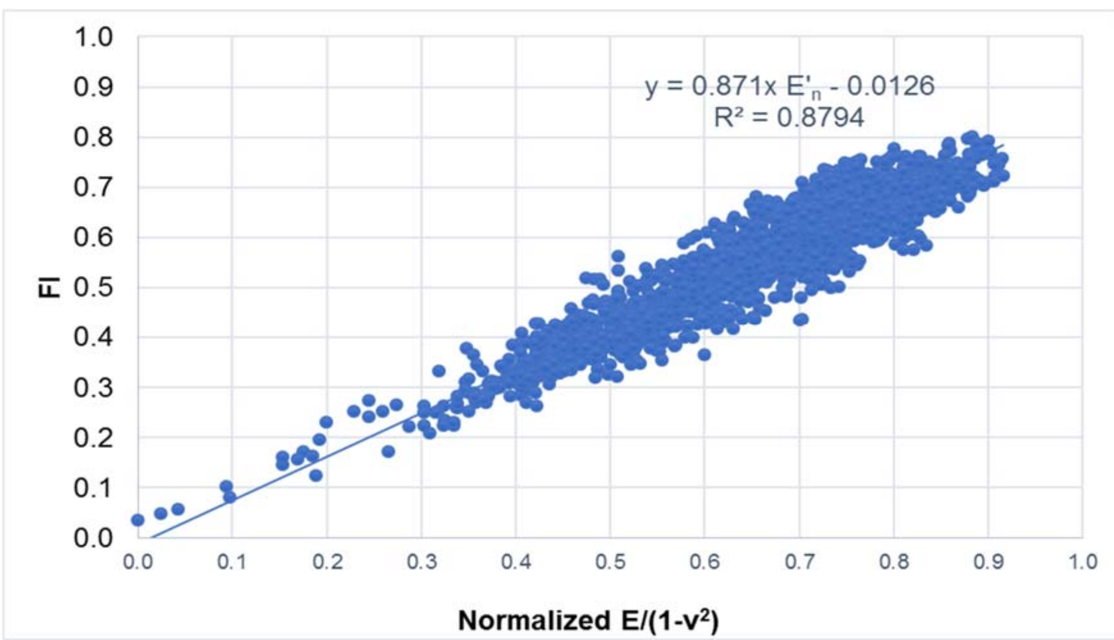

Figure 8: A geomechcanical based FI correlation introdued by Alzahabi et al. 2015

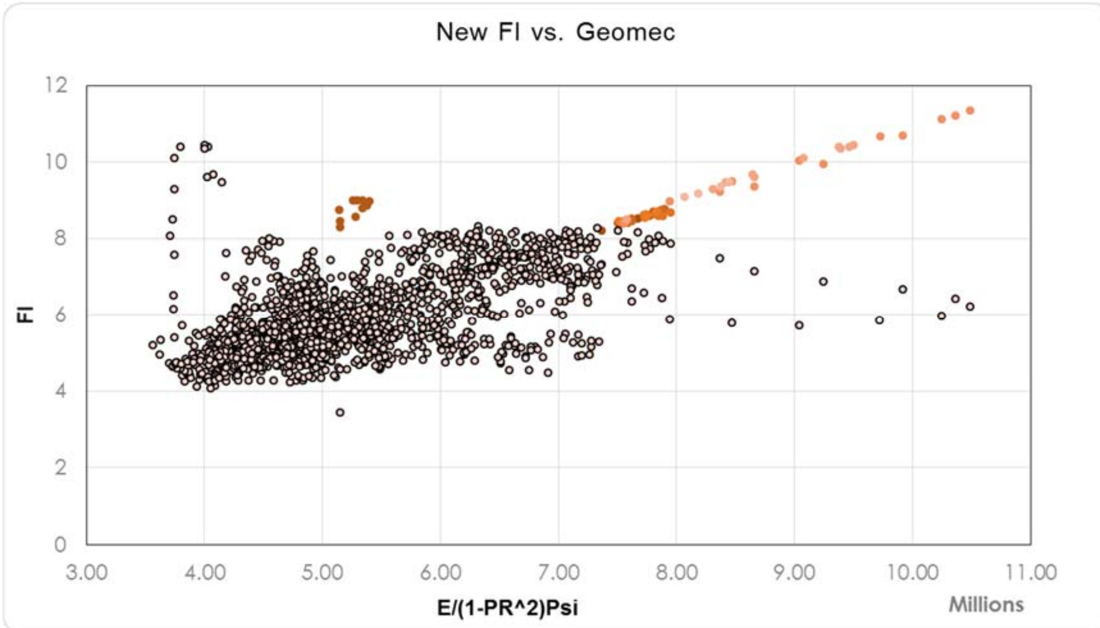

Figure 9: FI (2nd correlation) versus Plane Strain Young's Modulus

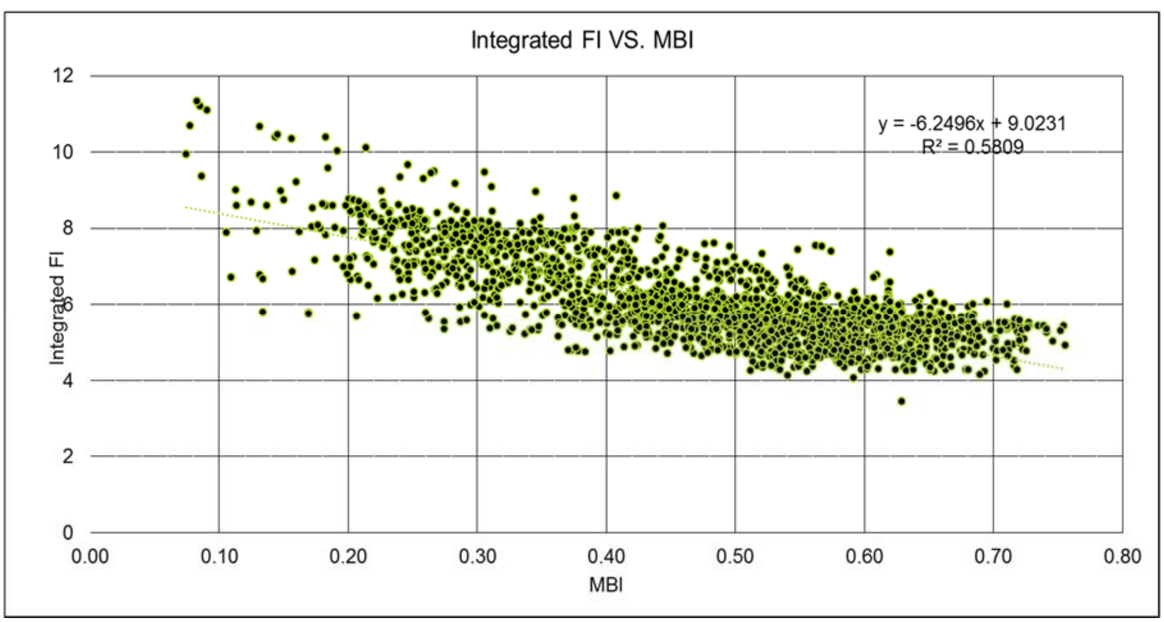

Figure 10: FI (2nd correlation) versus Mineralogical Brittleness Index

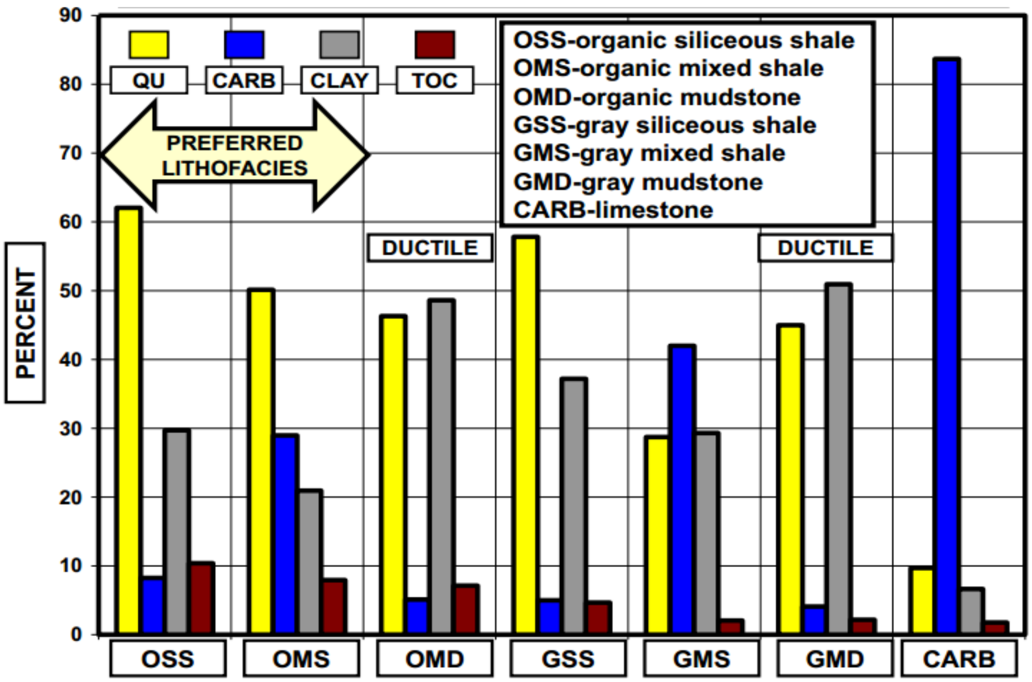

Figure 11: Marcellus Shale Lithofacies after Wang& Carr, 2013

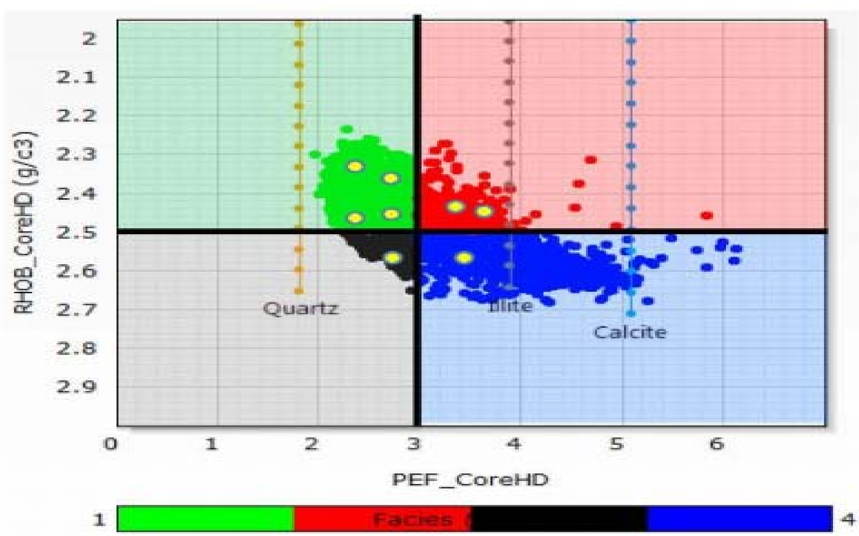

Figure 12: Four categories of sweet spot regions after Walls et al 2012

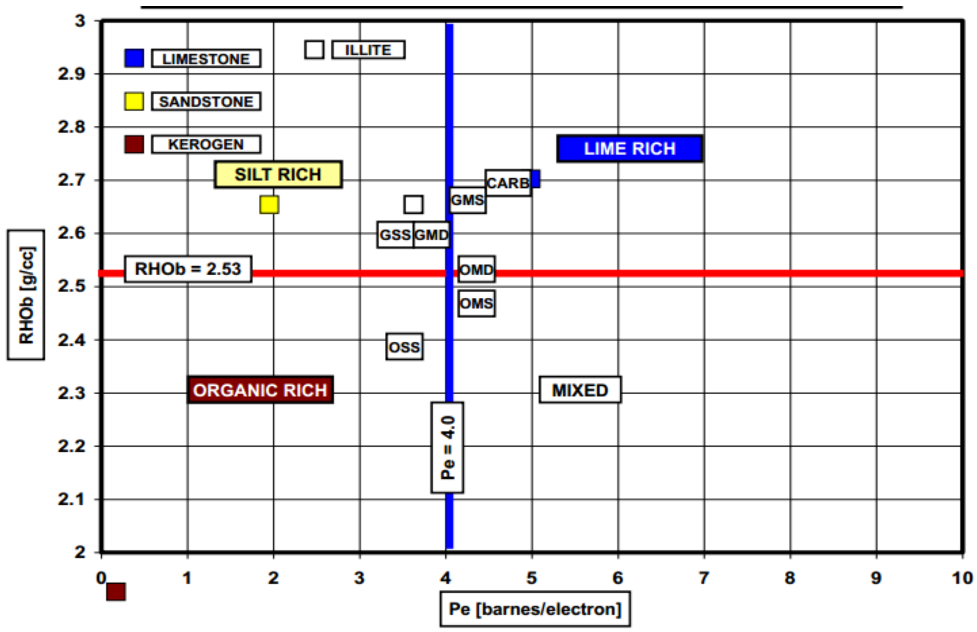

Figure 13: Shale

Lithofacies after Wang & Carr, 2013

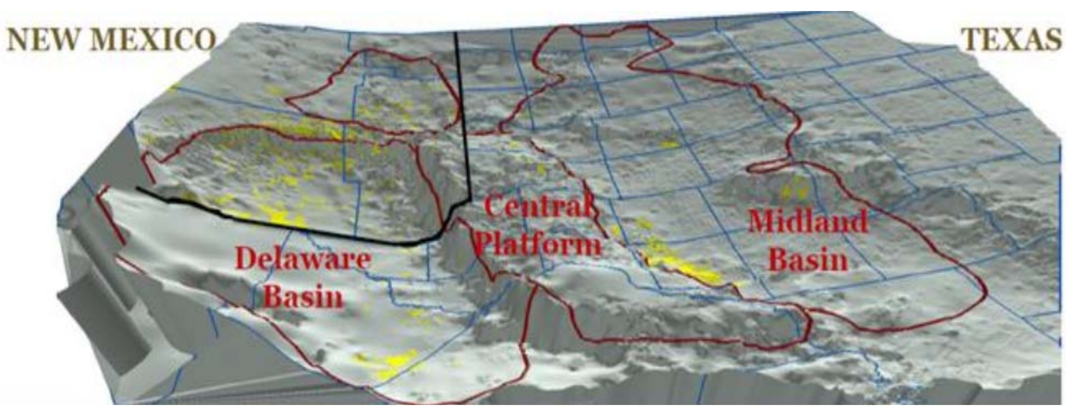

Figure 14: Map of a location of Permian Basin reservoir.

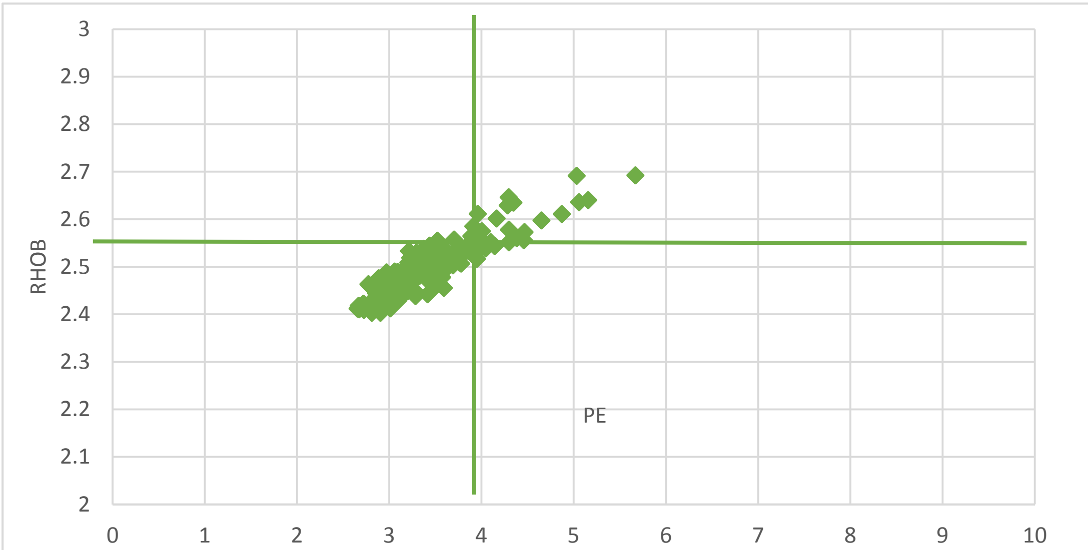

Figure 15: Selected zone Criteria 1

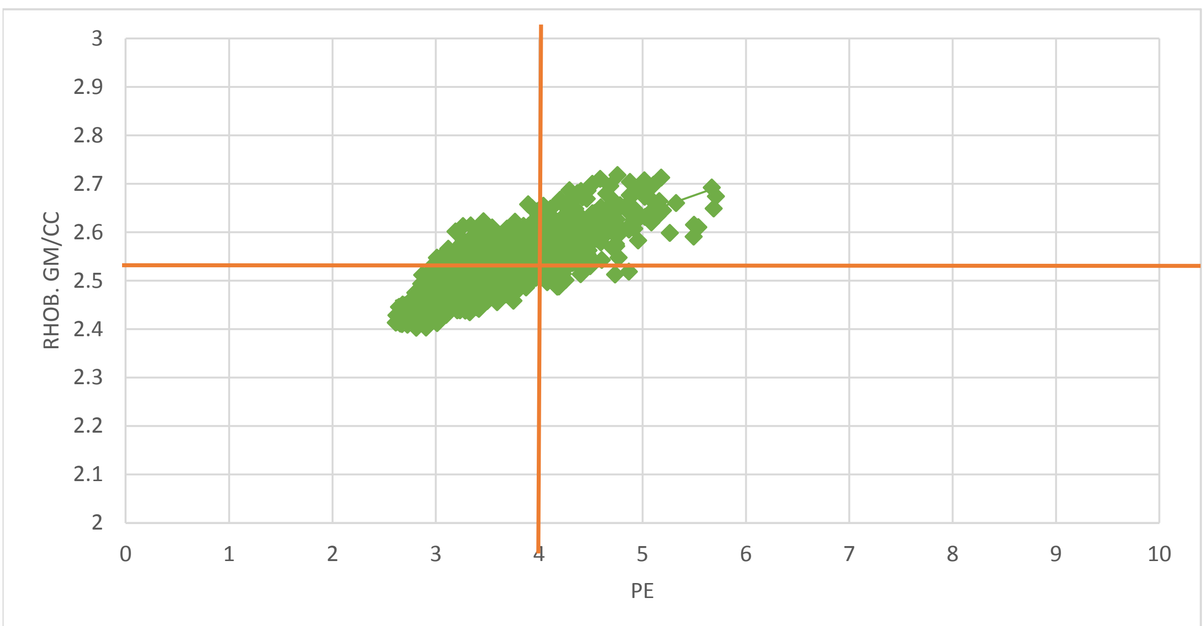

Figure 16: Shale Formation Criteria 1, 2 and 3

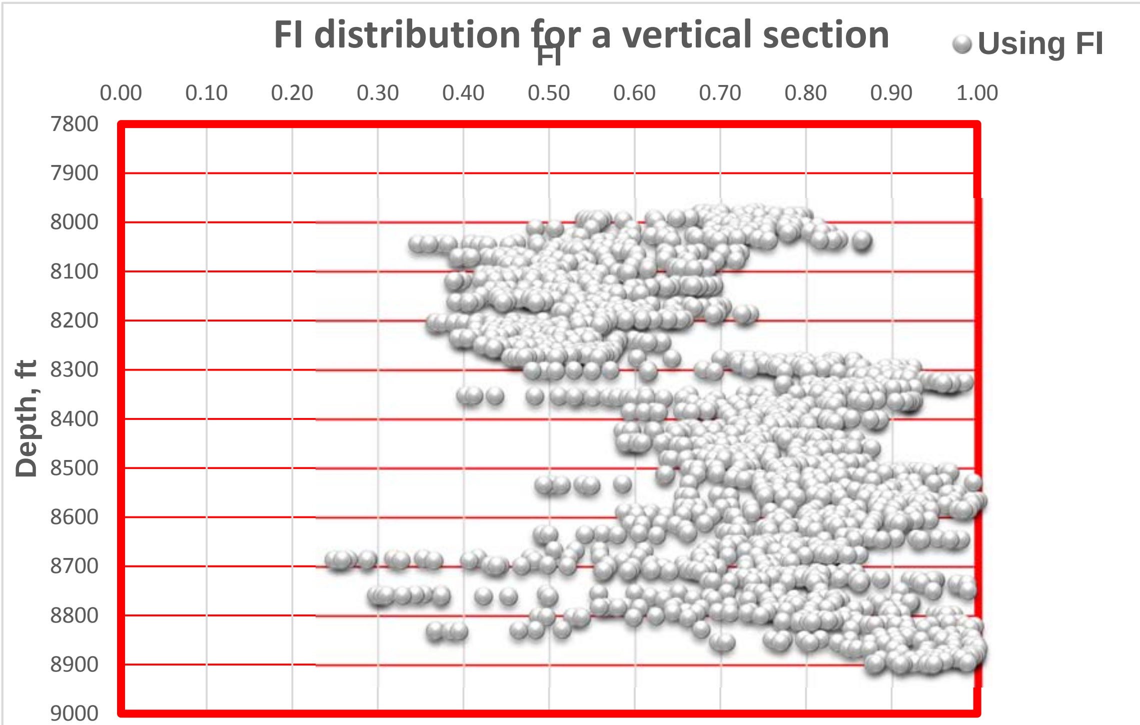

Figure 17: New developed FI versus depth

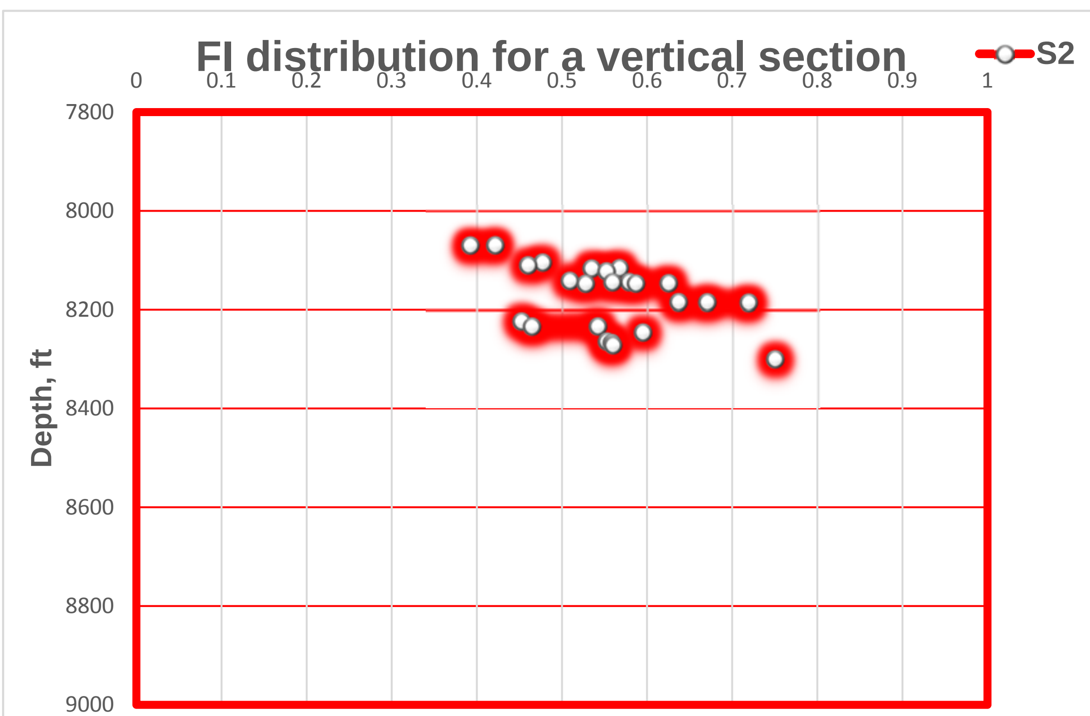

Figure 18: New developed FI screened by S1 conditions versus depth

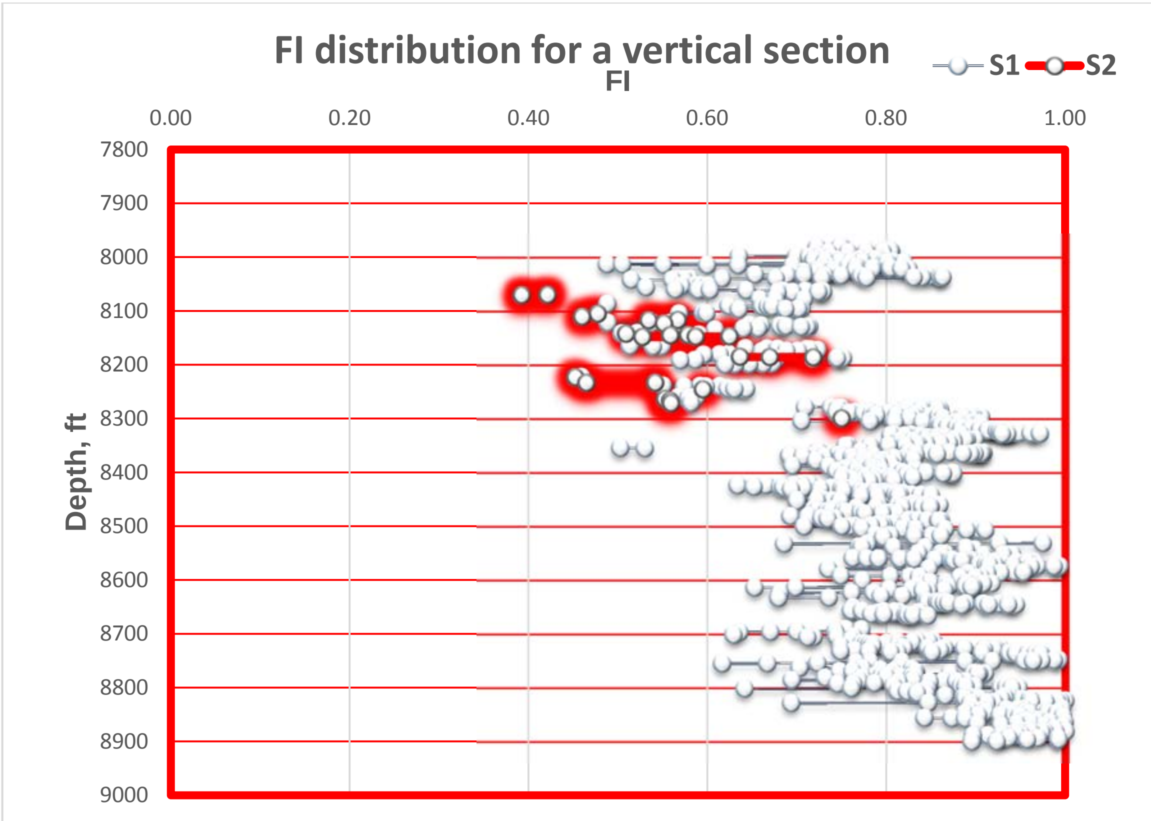

Figure 19: New developed FI screened by S1 and S2 conditions versus depth

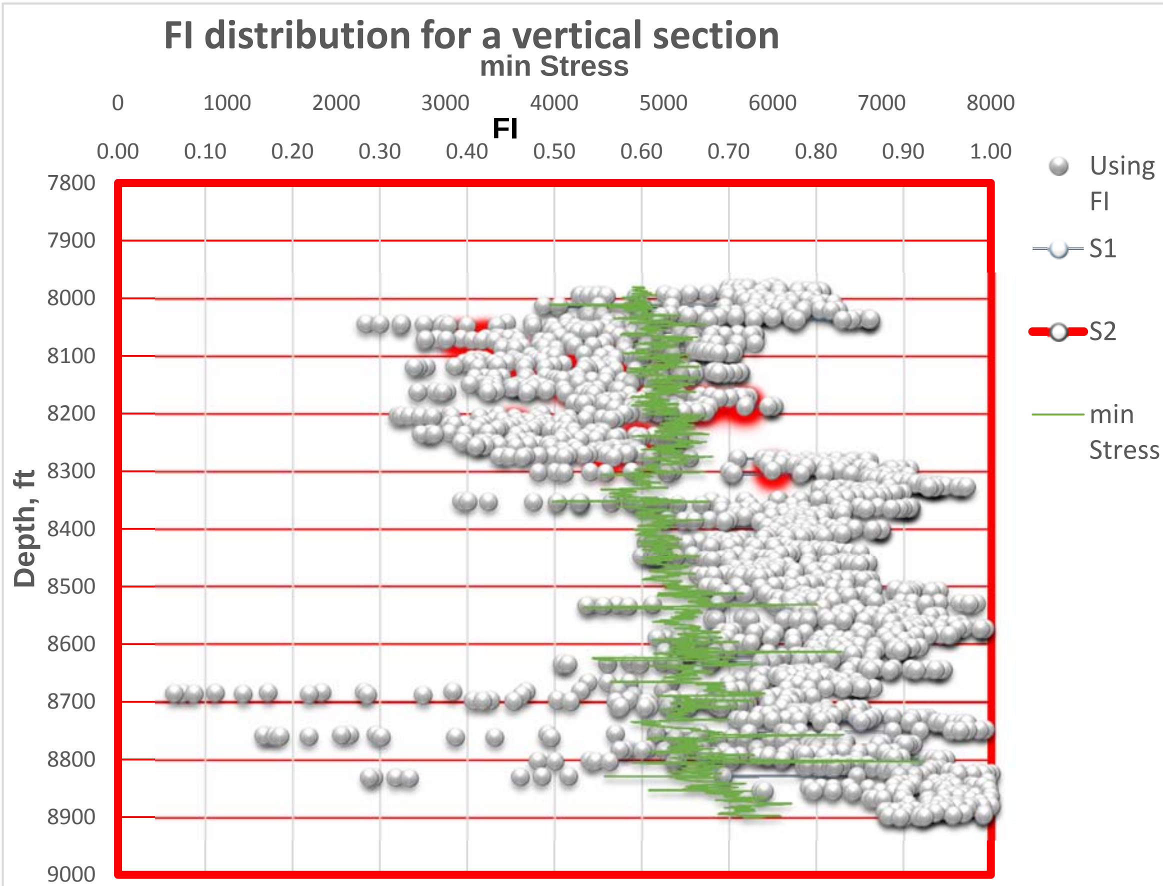

Figure 20: New developed FI screened by S1, S2 and min stress profile versus depth

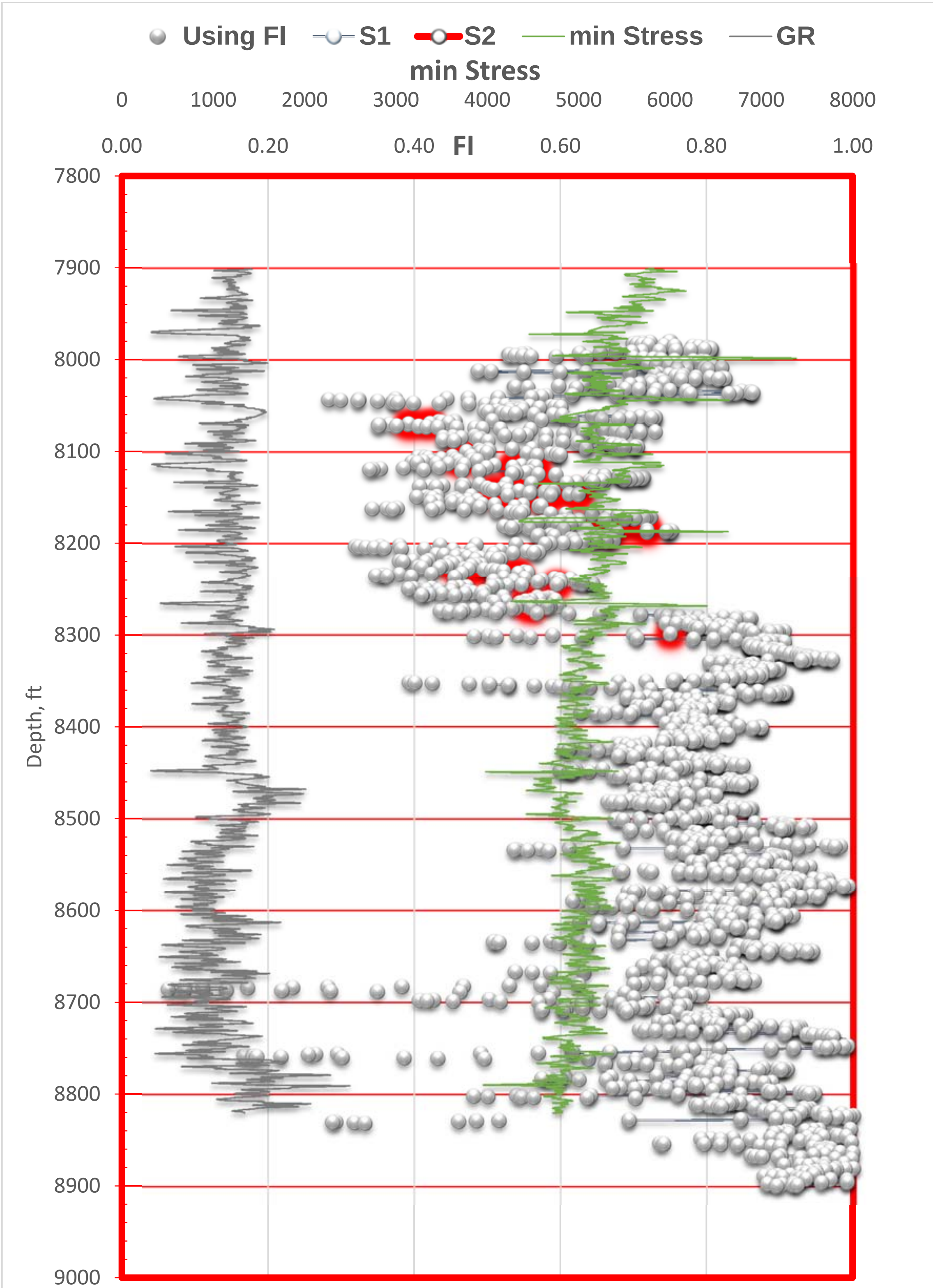

Figure 21: New developed FI screened by S1, S2 , min stress and gamma ray profile versus depth

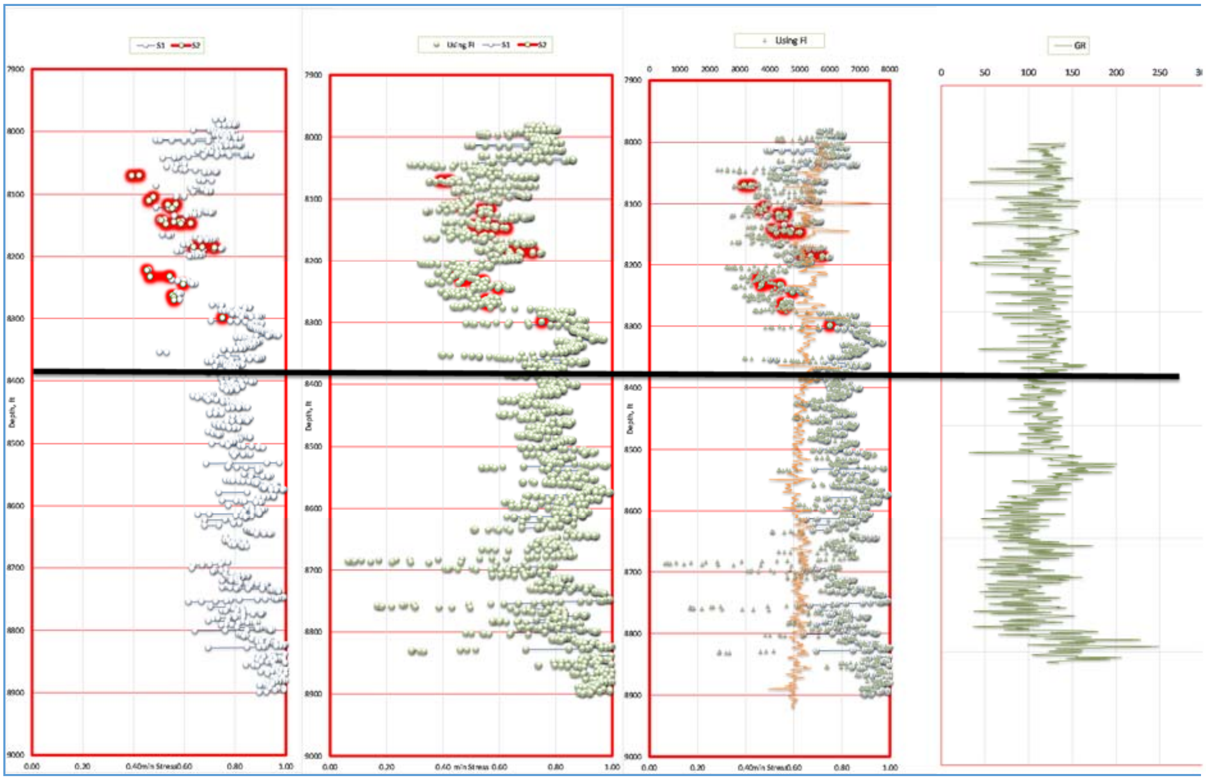

Figure 10: Permian Wolf Camp Shale : Midland basin Texas

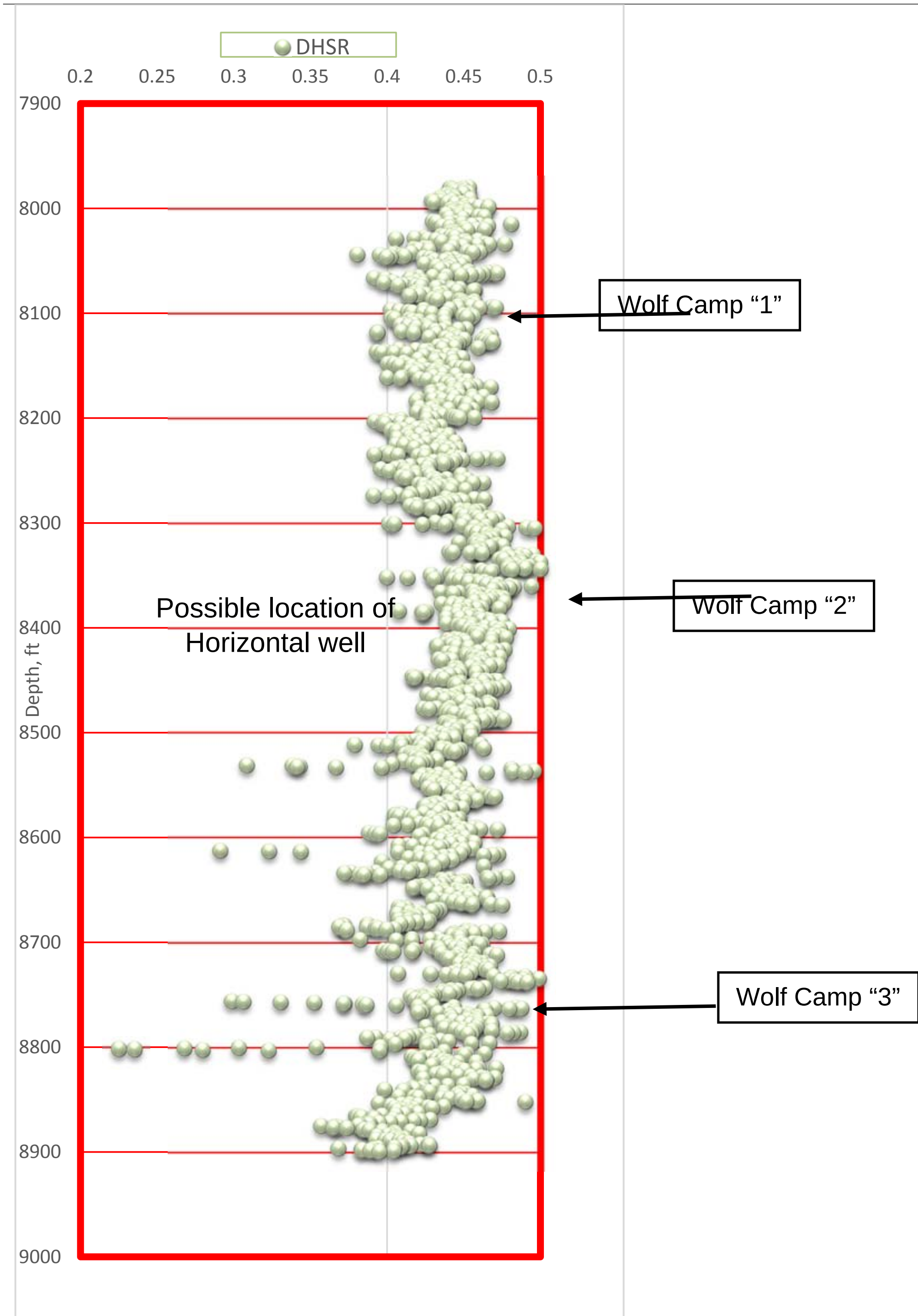

Figure 11: Differential Horizontal stress ratio versus depth.

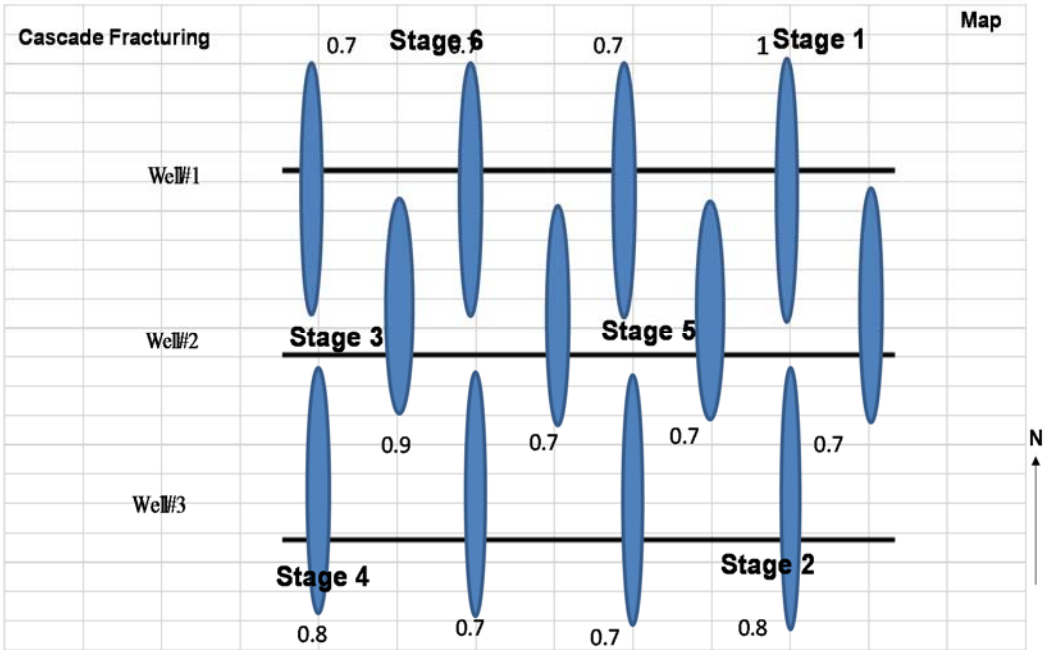

Figure 24: Schematic of a map view of suggested fracture stages suggested by FI values.

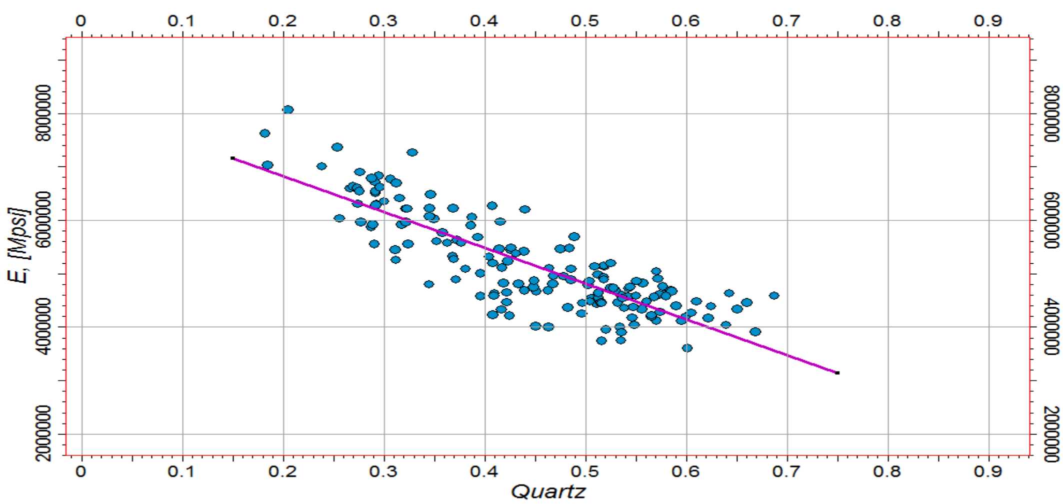

Figure 12: The relationship between Young's Modulus and Quartz of Wolf Camp Formation

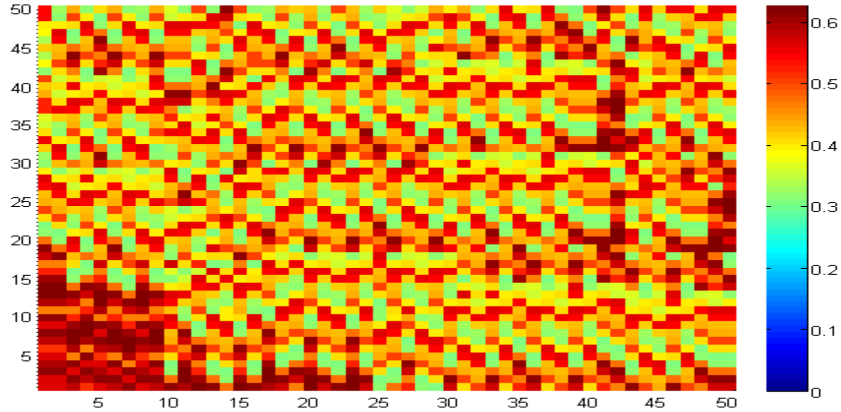

Figure 26: Fracturability Index map based on the tested shale model

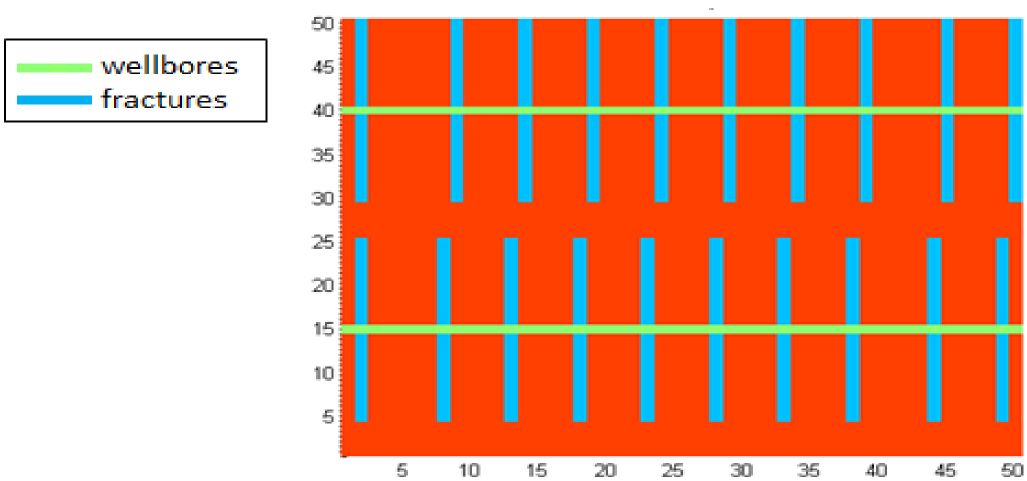

Figure 27: Optimal Placement for a Maximum Fracture Half-length of 10 and No Overlap

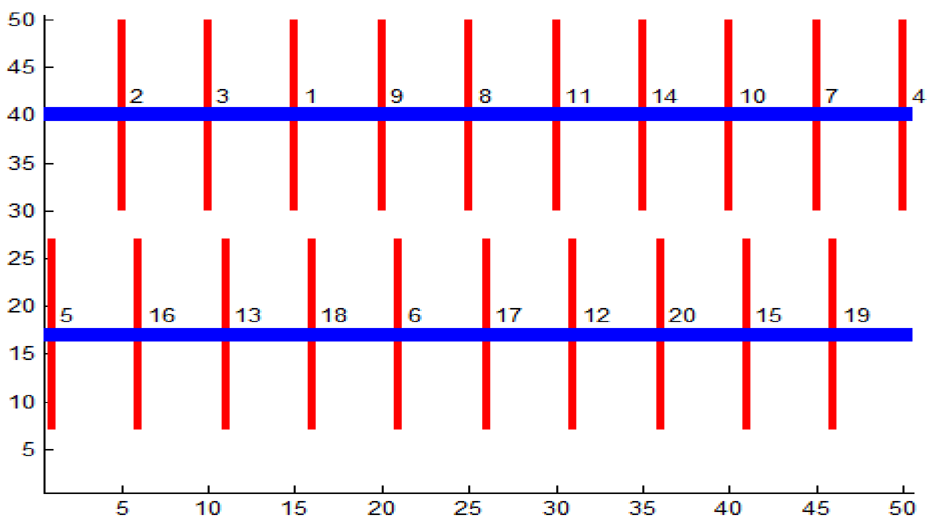

Figure 28: Sequencing of fractures according to FI values.